International Journal of Thermophysics, Vol. 11, No. 1, 1990

Pressure Effects on the Raman Spectra of 3-Deutero-Ammonia, Lattice Dynamics and Vibrons up to 40 GPa[1]

Ph. Pruzan,[2] M. Gauthier,[2] and J. C. Chervin[2]

High-pressure Raman studies up to 40 GPa have been made on solid ND_3 at room temperature. Features of external and internal modes are compared to that of solid NH_3 and mode assignments are proposed in solid phase IV ($p \geqslant 3.8$ GPa). In contrast with NH_3, which transforms to a cubic phase at 15 GPa, solid IV ND_3 was observed to be stable up to 40 GPa, the upper limit of the present investigation. It is concluded that bond symmetrization in ND_3 will occur above that of NH_3.

KEY WORDS: ammonia; deutero-ammonia; high pressure; hydrogen bond; Raman spectra.

1. INTRODUCTION

Application of pressure to a molecular solid reduces the intermolecular bond lengths and, in the case of H-bonded materials, causes the strenthening of the H bond and a corresponding stretching of the covalent bond length. Such a behavior, which is expected from structural studies at atmospheric pressure [1], was shown to occur under pressure for H_2O, HCL, HBr, HCOOH, and NH_3 solids [2–5].

This specific feature of H-bonded materials is of interest for (i) the understanding of the H-bond mechanism and (ii) the study of the change in crystal properties when symmetrization of the H bond occurs.

Using Raman scattering data, symmetrization of the H bond was shown to occur in NH_3 around 60 GPa [5]. Significant changes of the

---

[1] Paper presented at the Tenth Symposium on Thermophysical Properties, June 20–23, 1988, Gaithersburg, Maryland, U.S.A.

[2] Physique des Milieux Condensés (CNRS-UA 782), Université Pierre et Marie Curie, 4 Place Jussieu, F-75252 Paris Cedex 05, France.

internal vibration spectrum begin at 15 GPa, where the crystal symmetry transforms from hexagonal to cubic. These modifications are progressive with pressure and involve a transformation leading to a breaking down of the usual picture of the crystal composed of molecular entities. The resulting solid would be more like a covalent or a ionic solid.

In the present work, we report external and internal Raman spectra of solid ND_3 up to 40 GPa. By comparing with previous results on NH_3, assignments of lattice modes are provided. It is also observed that the effect due to deuterium isotope substitution is very marked. The high-pressure phase diagrams of NH_3 and ND_3 are different and symmetrization of ND_3 should occur well above that of NH_3.

2. EXPERIMENTAL

A new type of diamond cell (DAC) was used in this experiment. This DAC has been described in a recent paper by Le Toullec et al. [6]. The driving force on the sliding piston is exerted by fluid pressure on a steel membrane. The body of the cell is cylindrical, 50 mm in diameter and 50 mm in length. Anvils seats allow for a 2 × 15° angular opening for incident and scattered light.

The diameter of the diamond anvil culet was either 800 or 475 μm, depending on the maximum pressure of the investigation. The gasket hole was, respectively, 400 and 200 μm with an original thickness of about 40 μm. The sample space was filled by condensing liquid deuterated ammonia (CEA, Bureau des Isotopes stables; isotopic purity $\geqslant 99.75$) using an indium ring around the diamonds and crossed radially by a thin capillary. Raman spectra were recorded with a T 800 Coderg triple monochromator with a cooled photomultiplier and a photon-counting system. The instrumental resolution was 3 cm^{-1} with 300 μm slits. We used forward (0°) and backward (180°) scattering geometries. For one particular run a double monochromator with a multichannel analyzer (Microdil 28, Dilor) was used. The laser beam, 100 mW at the entrance of the DAC with the 488 nm line from an argon–ion laser, was focused down to a 10 μm spot on the sample.

Pressure was measured using the shift of the R_1 fluorescence line of 3000 ppm Cr^{3+} ruby chips placed in the sample space according to the Mao and Bell pressure scale [7].

3. RESULTS

At room temperature, liquid ammonia solidifies at 1 GPa to cubic ammonia III and then transforms around 3.8 GPa to hexagonal ammonia

IV. Comprehensive data and references for the low- and high-pressure phases were given in recent papers [5, 8]. The present work concerns the pressure region above 4 GPa.

It was found using x-ray technique that NH_3 solid IV is hexagonal with $P6_3/mmc$ (D_{6h}^4) symmetry [9]. According to our previous Raman analysis [5], the number of Raman-active modes leads to the conclusion that the site symmetry is 3m (C_{3v}). From group theoretical analysis the following species for the zone-center normal active Raman modes are expected: $1A_{1g} + 1E_{1g} + 1E_{2g}$ lattice translations; $1E_{1g} + 1E_{2g}$ lattice librations; and $\nu_1(A_{1g}) + \nu_3(E_{2g}) + \nu_3(E_{1g})$ internal modes in the region of the stretching modes. In the following, the same symmetry is assumed for ND_3 solid IV.

3.1. Phonons and Librons

The shift of frequencies of the lattice peaks, ν, with pressure, p, are shown in Fig. 1. Above 4 GPa, six external peaks were observed in solid

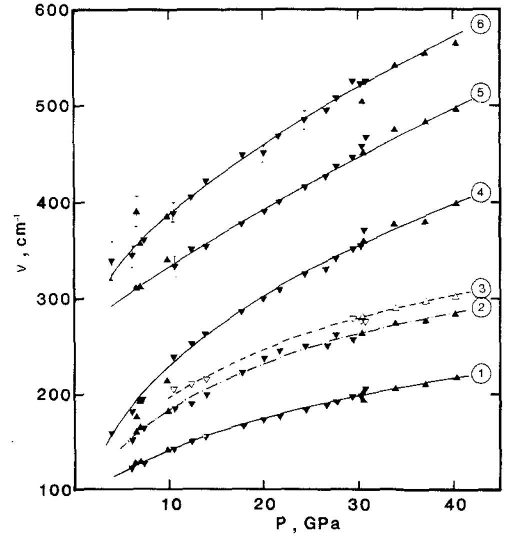

Fig. 1. Frequencies of the Raman lattice peaks of ND_3 solid IV as a function of pressure at $T = 300$ K. Peaks are numbered from 1 to 6 in order of increasing frequency. (▲) Increasing pressure runs; (▼) decreasing pressure runs; (△) peak number 3. Error bars are indicated when uncertainties are larger than $5\,cm^{-1}$. Solid lines, smooth curves; assignments are given in Table I.

ND_3, i.e., one more than in NH_3. Furthermore, in NH_3 slight jumps and changes of slope were observed around 15 GPa. In ND_3 no such features were observed, up to 40 GPa, the upper limit of the present investigation. For convenience, these peaks are numbered from 1 to 6 in order of increasing frequency. Apart from peaks 1 and 4, the modes appear as humps upon the background signal. Peaks 2 and 3 are very close together and are well resolved only above 30 GPa. Widths, slopes $d\nu/dp$, Grüneisen parameters, and the frequency shift factor on deuteration are given in Table I. It is to be noted that, between 4 and 40 GPa, the integrated intensities of peaks 1, 4, and 5 increase by a factor close to 10. To compute the Gruneisen parameters we have used an empirical equation of state (EOS) based on the x-ray data of Mills on NH_3 up to 6 GPa [9]. These parameters, which represent average values in the range 10–40 GPa, may be compared to that of NH_3 given in Table II.

3.1.1. *Phonons* (*Translations*)

Provided that the intermolecular force constants are the same in NH_3 and ND_3, translations may be identified by a frequency shift on deuteration by a factor of 1.085 [i.e., $(20/17)^{1/2}$]. Analysis of the present data compared to our previous results on NH_3 shows that the relevant ND_3 and NH_3 peaks are, respectively, 1, 2, and 4 and 1, 2, and 3 (Table II). Frequency ratios, given in Table I, are mean values over the range 10–30 GPa.

3.1.2. *Librons*

These modes originate from hindered rotations about either the molecular axis or the axis perpendicular to it. They may be identified by a

Table I. Characteristic Features of the Raman Lattice Modes of ND_3 Solid IV: Widths at 10 GPa, Mean Values of the Slopes $d\nu/dp$, and Grüneisen Parameters γ in the Range 10–40 GPa; Mean Values of the Frequency Ratio ν_{NH_3}/ν_{ND_3} in the Pressure Range 10–30 GPa

Peak No.	Assignment	Width (cm^{-1})	Slope ($cm^{-1} \cdot GPa^{-1}$)	γ	ν_{NH_3}/ν_{ND_3}
1	$T(A_1)$	10	2.53	1.23	1.14
2	T^a	20	3.33	1.24	1.07
3	R^b	20	3.6	1.26	1.53
4	T^a	20	5.67	1.59	1.07
5	R^b	30	5.46	1.15	1.30
6	Comb.^{n}	40	6.13	1.12	

[a] $T(E_{1g} + E_{2g})$.
[b] $R(E_{1g} + E_{2g})$.

Table II. Characteristic Features of the Lattice Modes of NH_3 Solids IV and V according to Our Previous Work [5]: Assignments; Mean Values of the Slopes *dv/dp* in the Pressure Range 5–15 GPa (Solid IV); Mean Values of the Slopes *dv/dp* in the Pressure Range 15–30 GPa (Solid V); Respective Values of the Grüneisen Parameter γ

Peak No.	Assignment		Slope ($cm^{-1} \cdot GPa^{-1}$)		γ	
	IV	V	IV	V	IV	V
1	$T(A_1)$	$T(A_1)$	≈ 4	2.85	0.93	1.57
2	T^a	T^b	≈ 7.4	4.5	1.53	1.32
3	T^a	T^b	9.1	5.2	1.4	1.34
4	R^a	R^b	6.6	6	0.86	1.36
5	R^a	R^b	7.7	3.6	0.7	0.56

[a] Solid IV, $T(E_{1g}+E_{2g})$. $R(E_{1g}+E_{2g})$.
[b] Solid V, $T(E+F_2)$, $R(E+F_2)$.

shift on deuteration by a factor close to 1.40 [i.e., $(I_{NH_3}/I_{ND_3})^{1/2}$]. Analysis of our data allows us to assign peaks 3 and 5 to these modes. The corresponding NH_3 peaks are, respectively, 4 and 5 (Table II). The respective frequency ratios are about 1.5 and 1.3.

Provided that the crystal symmetry is $P6_3/mmc$ and the site symmetry 3m, peak 6 cannot be attributed to a fundamental mode. The high frequency of this peak suggests a combination mode which very likely involves peaks 2 and 3, which have the same symmetry and are energetically close. It is to be noted that in solid I an extra peak at high frequency was also found [10]. Another possible explanation of the number of Raman lines is to invoke structures of lower symmetry.

3.2. Vibrons

Above 4 GPa, we previously found that the internal spectrum of NH_3 solid IV consists of three broad bands, the assignments of which were given above. Upon compression, line $\nu_3(E_{2g})$ was found to decrease in intensity, and from 15 to 21 GPa a modification occurs indicating a phase change [5]. This observation is consistent with the observed discontinuity of the slopes of the lattice modes at 15 GPa.

The internal spectrum of ND_3 is in the frequency range of 2300–2600 cm^{-1}. Therefore, the sample signal may be strongly perturbed by the second-order Raman spectrum of the diamond anvils. This was seen particularly in a forward-scattering setup used during one increasing and decreasing pressure run up to 15 GPa. We subsequently, have used a setup with a backward-scattering geometry which lowered the background from the anvils.

As in NH_3 the bending modes ν_2 and ν_4 of ND_3 were not observed. Spectra of the stretching modes ν_1 and ν_3 are shown for four different pressures in Fig. 2. The pressure dependence of these frequencies is presented in Fig. 3. Close to 4 GPa, the internal spectrum of ND_3 looks like that of NH_3. However, upon further compression the spectrum evolves in a quite different way and, in particular, does not exhibit the features found for NH_3 between 14 and 22 GPa. One feature of the ND_3 spectrum is the continuous increase in the intensity of the $\nu_3(E_{2g})$ band, whereas a shoulder appears from 15 GPa on the high-energy side of the $\nu_3(E_{1g})$ peak. This rather continuous change of the internal spectrum is consistent with the observed behavior of the lattice modes. A second and striking feature of this spectrum is the very weak pressure dependence of the $\nu_1(A_{1g})$ peak compared to that of NH_3. In the range 4–40 GPa the experimental curve $\nu_1(A_{1g})$ is roughly flat, whereas that of NH_3 decreases by about 95 cm^{-1}. Actually this peak in ND_3 increases slightly to reach a maximum of about 18 GPa and then decreases.

The higher-frequency peaks $\nu_3(E_{2g})$ and $\nu_3(E_{1g})$ correspond respectively to the out-of-phase and the in-phase couplings between molecules in

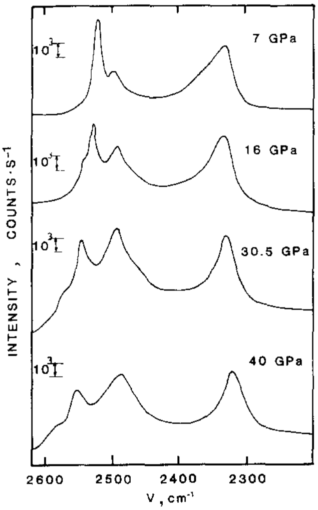

Fig. 2. Internal spectra of ND_3 solid IV for four different pressures. Assignments of the peaks in accord with a crystal symmetry $P6_3/mmc$ and a site symmetry 3m.

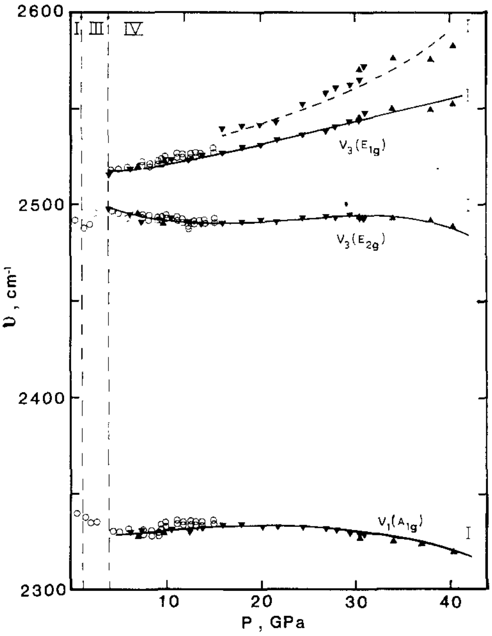

Fig. 3. Frequencies of the internal Raman peaks (stretching modes) of ND_3 solid IV as a function of pressure at $T = 300$ K. (▲) Increasing pressure runs; (▼) decreasing pressure runs; (○) run up to 15 GPa. Assignments of the peaks in accord with a crystal symmetry $P6_3/mmc$ and a site symmetry 3m. Error bar on the left.

the same cell. Since the E_{1g} mode is twofold degenerate, it is tempting to assume that pressure inhomogeneities cause splitting of that mode. Taking into account the behavior of the other modes, a phase change is not likely to be present.

4. DISCUSSION

As mentioned in the beginning, a characteristic feature of *H*-bonded compounds, such as those with O—H———0 bonds, is the stretching of the covalent length O—H as the d_{O-O} distance decreases. This property is directly correlated to the decrease of the ν_{O-H} frequency as d_{O-O} decreases. This effect has been systematically studied at atmospheric pressure using different molecules to obtain different bond distances [1]. Data indicate that for d_{O-O} close to 2.4 Å, the hydrogen bond lies midway between the two oxygens. A similar correlation for systems with

N—H———N bonds indicates a critical d_{N-N} distance of about 2.6 Å [11]. Infrared band shape analysis in solid imidazol provides the same d_{N-N} value [12].

A related effect is obtained by applying pressure on the same compound. For example, investigation on ice VIII lead to the conclusion that symmetrization occurs very likely around 47.5 GPa, where d_{O-O} is close to 2.4 Å [2]. Using Raman scattering we have recently found evidence for symmetrization of NH_3 around 60 GPa, where d_{N-N} is expected to be about 2.6 Å [5]. Significant and also gradual changes of the internal spectrum of NH_3 provide evidence for a change of the symmetry around one N involving ultimately six H nearest neighbors. Due to geometrical conditions, such a continuous change, which leads to a solid with symmetric bonds, is consistent with a cubic crystal symmetry found in fact above 15 GPa.

The main result of the present study is the marked difference between the Raman modes of NH_3 and ND_3 at high pressure. Our present investigation does not show any phase transition in ND_3 in the range 4–40 GPa. Furthermore, the pressure dependences of the ν_1 mode are quite different. In the following we show from a qualitative point of view that both points are strongly correlated.

It is generally agreed that a one-dimensional system, O—H———O, for example, may be represented by an asymmetric double-well potential [1]. As d_{O-O} decreases, the potential due to the H bond increases and the O—H frequency shifts toward lower frequency. Simultaneously the equilibrium position of the proton moves toward the midpoint. From a qualitative viewpoint the difference between nondeuterated and deuterated compounds arises from the difference in vibrational amplitudes of the O—H and O—D oscillators. This makes the proton more sensitive to the H bond changes than deuteron. Actually, it is known that H bond weakens on deuteration. It has been shown recently that a more comprehensive description of deuteration effect must take into account tunneling motion across the potential barrier between the two oxygens [13–15]. For example, a one-dimensional model using a symmetric double Morse potential leads to a sensitive difference between the d_{O-H} and the d_{O-D} distances for the same d_{O-O} length [14, 15]. Because of the weakness of the H bond in NH_3, the tunneling effect is very weak for the deuteron. This may involve for NH_3 and ND_3 a significant difference between equilibrium distances d_{N-H} and d_{N-D} and, consequently, for the same d_{N-N} distance, a smaller molecular distortion for the deuterated compound compared to the hydrogenated compound. This very likely accounts for the stability of ND_3 solid IV at least up to 40 GPa and also indicates a transition to a symmetrically bonded solid at a pressure higher than for NH_3.

ACKNOWLEDGMENTS

We would like to thank J. P. Pinceaux for very useful help in mounting and using the new type of diamond anvil cell. Helpful discussions with J. M. Besson and F. Fillaux are gratefully acknowledged.

REFERENCES

1. A. Novak, in *Structure and Bonding, 18*, J. H. Furhop, G. Blauer, T. J. R. Weakly, and A. Novak, eds. (Springer, Berlin, 1974), p. 177.
2. K. R. Hirsch and W. B. Holzapfel, *Phys. Lett.* **101A**:142 (1984); K. R. Hirsch and W. B. Holzapfel, *J. Chem. Phys.* **84**:2771 (1986).
3. R. A. Noak and W. B. Holzapfel, in *High Pressure Science and Technology*, K. D. Timmerhaus and M. S. Barber, eds. (Plenum Press, New York, 1979), Vol 1, p. 748; P. G. Johansen, W. Helle, and W. B. Holzapfel, in *J. Phys.* **C8** Suppl. **11**:199 (1984).
4. H. Shimizu, *Physica* **139/140B**:479 (1986).
5. M. Gauthier, Ph. Pruzan, J. C. Chervin, and J. M. Besson, *Phys. Rev. B* **37**:2102 (1988).
6. R. Le Toullec, J. P. Pinceaux, and P. Loubeyre, *High Press. Res.* **1**:77 (1988).
7. H. K. Mao, P. M. Bell, J. W. Shaner, and D. J. Steinberg, *J. Appl. Phys.* **49**:3276 (1978).
8. J. Eckert, R. L. Mills, and S. K. Satija, *J. Chem. Phys.* **81**:6034 (1984).
9. R. L. Mills, Private Communication.
10. D. S. Binbrek and A. Anderson, *Chem. Phys. Lett.* **15**:421 (1972).
11. T Gloviak, E. Grech, Z. Malarski, and L. Sobczyk, *J. Mol. Struct.* **177**:339 (1988).
12. F. Fillaux, Private communication.
13. K. S. Schweizer and F. H. Stillinger, *J. Chem. Phys.* **80**:1230 (1984).
14. E. Matshushita and T. Matsubara, *Prog. Theor. Phys.* **67**:1 (1982).
15. M. Mackowiak, *Physica* **145B**:320 (1987).